



# The inhibitory receptor CD94/NKG2A on CD8<sup>+</sup> tumor-infiltrating lymphocytes in colorectal cancer: a promising new druggable immune checkpoint in the context of HLA-E/ $\beta$ 2m overexpression

Juliette Eugène<sup>1</sup> · Nicolas Jouand<sup>2,3</sup> · Kathleen Ducoin<sup>2,3</sup> · Delphine Dansette<sup>1</sup> · Romain Oger<sup>2,3</sup> · Cécile Deleine<sup>2,3</sup> · Edouard Leveque<sup>2,3</sup> · Guillaume Meurette<sup>4,5</sup> · Juliette Podevin<sup>4</sup> · Tamara Matysiak<sup>4,5</sup> · Jaafar Bennouna<sup>4,5</sup> · Stéphane Bezieau<sup>5,6</sup> · Christelle Volteau<sup>7</sup> · Wassila El Alami Thomas<sup>8</sup> · Jérôme Chetritt<sup>8</sup> · Olivier Kerdraon<sup>9</sup> · Pierre Fourquier<sup>10</sup> · Emilie Thibaudeau<sup>11</sup> · Frédéric Dumont<sup>11</sup> · Jean-François Mosnier<sup>1,5</sup> · Claire Toquet<sup>1,5</sup> · Anne Jarry<sup>2,3</sup> · Nadine Gervois<sup>2,3</sup> · Céline Bossard<sup>1,2,3,5</sup>

Received: 28 March 2019 / Revised: 13 June 2019 / Accepted: 14 June 2019 / Published online: 13 August 2019  
© United States & Canadian Academy of Pathology 2019

## Abstract

We previously demonstrated that HLA-E/ $\beta$ 2m overexpression by tumor cells in colorectal cancers is associated with an unfavorable prognosis. However, the expression of its specific receptor CD94/NKG2 by intraepithelial tumor-infiltrating lymphocytes, their exact phenotype and function, as well as the relation with the molecular status of colorectal cancer and prognosis remain unknown. Based on a retrospective cohort of 234 colorectal cancer patients, we assessed the expression of HLA-E,  $\beta$ 2m, CD94, CD8, and NKp46 by immunohistochemistry on tissue microarray. The expression profile of HLA-E/ $\beta$ 2m on tumor cells and the density of tumor-infiltrating lymphocytes were correlated to the clinicopathological and molecular features (Microsatellite status, *BRAF* and *RAS* mutations). Then, from the primary tumors of 27 prospective colorectal cancers, we characterized by multiparameter flow cytometry the nature (T and/or NK cells) and the co-expression of the inhibitory NKG2A or activating NKG2C chain of ex vivo isolated CD94<sup>+</sup> tumor-infiltrating lymphocytes. Their biological function was determined using an in vitro redirected cytolytic activity assay. Our results showed that HLA-E/ $\beta$ 2m was preferentially overexpressed in microsatellite instable tumors compared with microsatellite stable ones (45% vs. 19%, respectively,  $p = 0.0001$ ), irrespective of the *RAS* or *BRAF* mutational status. However, HLA-E/ $\beta$ 2m<sup>+</sup> colorectal cancers were significantly enriched in CD94<sup>+</sup> intraepithelial tumor-infiltrating lymphocytes in microsatellite instable as well as in microsatellite stable tumors. Those CD94<sup>+</sup> tumor-infiltrating lymphocytes mostly corresponded to CD8<sup>+</sup>  $\alpha\beta$  T cells, and to a lesser extent to NK cells, and mainly co-expressed a functional inhibitory NKG2A chain. Finally, a high number of CD94<sup>+</sup> intraepithelial tumor-infiltrating lymphocytes in close contact with tumor cells was independently associated with a worse overall survival. In conclusion, these findings strongly suggest that HLA-E/ $\beta$ 2m–CD94/NKG2A represents a new druggable inhibitory immune checkpoint, preferentially expressed in microsatellite instable tumors, but also in a subgroup of microsatellite stable tumors, leading to a new opportunity in colorectal cancer immunotherapies.

## Introduction

In colorectal cancers, an improved prognosis has been associated with a high number of memory and cytotoxic T lymphocytes in primary tumors [1, 2], independently of the pathological tumor node metastasis (pTNM) stage, as well as with a high number of tumor-specific T cells [3]. The major prognostic impact of this immunoscore in non metastatic colorectal cancers, recently validated by a large international consortium [4], strongly suggests a link between tumor development/progression and in situ T-cell responses and gives diverse therapeutic opportunities for

These authors contributed equally: Juliette Eugène, Nicolas Jouand

These authors contributed equally: Nadine Gervois, Céline Bossard

**Supplementary information** The online version of this article (<https://doi.org/10.1038/s41379-019-0322-9>) contains supplementary material, which is available to authorized users.

✉ Céline Bossard  
celine.bossard@chu-nantes.fr

Extended author information available on the last page of the article

enhancing antitumor immunity in a tumor currently considered as immunogenic. This host immune response is more pronounced in microsatellite instable colorectal cancers, representing 15% of all colorectal cancers, compared with microsatellite stable colorectal cancers, probably due to a huge number of frameshift and missense mutations giving rise to a high number of immunogenic neo-epitopes in microsatellite instable colorectal cancer [5, 6]. Recent transcriptomic studies have clearly isolated microsatellite instable colorectal cancers, in part defined by an increased expression of Th1- and cytotoxic T lymphocytes-associated genes [7, 8]. However, this strong Th1/cytotoxic T lymphocytes gene signature is associated with an overexpression of immune inhibitory receptors, ligands, and metabolic enzymes, such as PD-1, Lag3, CTLA-4, PD-L1, and IDO-1 [5, 7, 9, 10]. These latter findings indicate that the immune microenvironment, able to recognize immunogenic antigens in microsatellite instable colorectal cancers, is unfortunately strongly counterbalanced by several inhibitory immune checkpoints. A better understanding of these ligand–receptor interactions that can be blocked by antibodies is crucial for the design of novel immune-based therapies in this field of oncology.

Interestingly, *in vitro* studies suggested that overexpression of HLA-E, a poorly polymorphic human MHC class Ib molecule, featuring a narrow tissue distribution but a low-cell surface expression, could be a mechanism of immune escape in various tumor types such as glioma, melanoma, or colorectal cancer [11–13]. Indeed, via aberrant overexpression by tumor cells, HLA-E can induce a tolerogenic effect on immune effector cells after engagement of the CD94/NKG2A (Natural killer group 2A) inhibitory receptor. The biological activity of HLA-E requires co-expression of the light chain  $\beta 2$  microglobulin ( $\beta 2m$ ) to form a stable heterodimer—HLA-E/ $\beta 2m$ —that interacts preferentially either with the CD94/NKG2A inhibitory receptor or the CD94/NKG2C (Natural killer group 2C) activating receptor [14]. These receptors are mainly expressed by NK cells, but also by a fraction of T cells (CD8 $\alpha\beta$  and  $\gamma\delta$  T cells) [15]. We previously demonstrated that 20% of colorectal cancers overexpress HLA-E/ $\beta 2m$  by tumor cells, and that this overexpression is significantly associated with a worse prognosis [16]. These findings suggest that HLA-E/ $\beta 2m$  overexpression in colorectal cancer could allow tumor cells to escape immune surveillance favoring tumor progression. In this context, the current study aims at assessing in a large cohort of primary resected colorectal cancer patients, (i) the expression profile of HLA-E/ $\beta 2m$  on tumor cells and the density of CD94<sup>+</sup> tumor-infiltrating lymphocytes in relation with the clinicopathological and molecular features of colorectal cancer, (ii) the nature (T and/or NK cells), phenotype (co-expression of the inhibitory NKG2A

or activating NKG2C chain), and biological function of CD94<sup>+</sup> tumor-infiltrating lymphocytes, and finally (iii) their prognostic influence.

## Materials and methods

### Patients

A total of 234 consecutive patients treated for a sporadic colorectal cancer at the Department of Surgery between 1998 and 2014 (Centre Hospitalier Universitaire, Nantes, France), without previous chemotherapy or radiotherapy, were included retrospectively in this study (cohort 1). We previously determined the status of HLA-E/ $\beta 2m$ , as well as the density of CD8<sup>+</sup> intraepithelial tumor-infiltrating lymphocytes and collected the clinical data for 80 patients of this cohort [16]. Taking into account the loss to follow-up of some elderly patients, the unknown cause of death for many of those patients, and the known negative impact of an advanced age on survival [17], we restricted survival analyses to patients under 75 years of age ( $n = 130$ ). The choice of this cut-off was based on the French colorectal cancer screening campaign that concerns only persons less than 75 years of age. For flow cytometry and functional analyses, a second cohort of 27 additional patients (cohort 2) undergoing surgery for colorectal cancer at the Department of Digestive Surgery of the Centre Hospitalier Universitaire of Nantes, Institut de Cancerologie de l'Ouest or Nouvelles Cliniques Nantaises of Nantes was included. For those 27 patients, tissue fragments of both primary tumor and macroscopically normal colonic mucosa taken 10 cm downstream the tumor, were cut out from the surgical colectomy. Peripheral blood obtained at the same time as the colectomy allowed isolation of peripheral blood mononuclear cells. Pathological staging of all patients was assessed according to the eighth edition of the TNM staging system for colorectal cancer published by the International Union against Cancer (UICC eighth edition). The histological subtyping was reviewed according to the fourth edition of World Health Organization classification of tumors of the digestive system.

All tissues were processed according to the guidelines of the French Ethics Committee for research on human tissues. The institutional board of the University Hospital of Nantes approved this study. Our tissue biocollection has been registered with the French Ministry for Higher Education and Research (DC-2014-2206) with approval from the ethic committee (CPP Ouest IV—Nantes). Our study was conducted in accordance with the Helsinki Declaration. Each patient included in this study signed an informed consent form.

## Microsatellite instability and DNA mismatch repair status

Microsatellite instability or mismatch repair statuses were performed as part of the diagnosis or for the purpose of the study by polymerase chain reaction (PCR) or immunohistochemistry, respectively (25 tumors were tested by immunohistochemistry only, the remaining by immunohistochemistry and PCR). The microsatellite instability status was determined using a pentaplex PCR with five markers: BAT-25, BAT-26, NR-21, NR-22, and NR-24 [18]. Briefly, genomic DNA was extracted from 10  $\mu\text{m}$  thick tissue sections of formalin-fixed, paraffin-embedded colorectal tumor tissue after manual macrodissection using iPrep™ ChargeSwitch® Forensic kit (Invitrogen), and according to the manufacturer's instructions. A colorectal cancer was considered as microsatellite unstable if at least 2 of these 5 markers showed microsatellite instability [19]. The mismatch repair status was assessed by immunohistochemistry using the following antibodies: MLH1 (clone ES05, Dako), MSH2 (clone FE11, Dako), MSH6 (clone EP49, Dako), and PMS2 (clone EP51, Dako).

## Tissue microarray construction

For the retrospective cohort, representative areas of tumor and paired normal colonic mucosa were carefully selected from hematoxylin and eosin stained sections. Four tissue cores (1 mm in diameter) were obtained for each case, three from the tumor (invasive front and center) and one from normal colonic mucosa. The tissue cores were then inserted in a recipient paraffin block. Each tissue microarray contained one core of normal placenta that served as a positive control.

## Quantitative immunohistochemistry

Immunohistochemistry was performed on 5  $\mu\text{m}$  formalin-fixed paraffin embedded sections from each tissue microarray described above, with an automated stainer (AutostainerLink 48, DAKO). Slides were stained with the following primary antibodies: HLA-E (clone MEM-E/02, dilution 1:50, Serotec),  $\beta\text{2m}$  (dilution 1:200, gift of Joelle Gachet, U892, Nantes), CD8 (clone C8/144B, dilution 1:50, Dako), CD94 (clone B-D49, 1:20, Diaclone), and NKp46 (clone 195314, 1:100, R&D systems). The immunological reactions were visualized with the Envision detection system (Dako). A strong membranous and cytoplasmic co-expression of HLA-E and  $\beta\text{2m}$  by tumor cells (profile considered as a stable and functional membrane HLA-E expression) was considered as an overexpression of HLA-E/ $\beta\text{2m}$  compared with no or faint co-expression of HLA-E and  $\beta\text{2m}$  by epithelial cells from normal colonic mucosa [16]. A colorectal cancer was considered as positive if at

least 5% of tumor cells overexpressed HLA-E (a threshold we previously used in our first study, and associated with a worse prognosis) [16] and  $\beta\text{2m}$  considering the three spots of tumor for each case. The density of intraepithelial tumor-infiltrating lymphocytes expressing CD8, CD94 and NKp46 was estimated by counting the number of positive cells per 100 epithelial cells in three different fields at  $\times 200$  magnification, corresponding to the surface of a spot of tissue microarrays.

## Immunofluorescence study

To assess the co-expression of CD94 and NKG2A by intraepithelial tumor-infiltrating lymphocytes, we performed an immunofluorescence analysis on frozen section of two colorectal cancers, one microsatellite unstable, and one microsatellite stable, chosen for their high density of CD94<sup>+</sup> intraepithelial tumor-infiltrating lymphocytes. Twelve micrometer thick cryostat sections were fixed in acetone. Double immunostaining was performed in two successive stages, using primary antibodies directed to CD94 (mouse monoclonal antibody, clone B-D49, Diaclone) and NKG2A (mouse monoclonal antibody, clone Z199, Beckman Coulter). Sections were first incubated with the anti-NKG2A antibody during 1 h and then after a phosphate-buffered saline (PBS) wash, with the Alexa Fluor 488-conjugated anti-mouse antibody (Invitrogen) for 30 min. After washing and fixation with 1% paraformaldehyde, sections were then incubated with the anti-CD94 antibody during 1 h and after a PBS wash, with the Alexa Fluor 647-conjugated anti-mouse antibody (Invitrogen) for 1 h. Nuclei were stained with DAPI. Sections were mounted using Prolong anti-fade medium (Molecular Probes). The fluorescence was observed on a fluorescent microscope (Axiovert 200-M, Carl Zeiss), equipped with an ApoTome slider, which eliminates image blurring. Image processing was performed using an AxioCam MR CCD camera and the Axiovision software (Carl Zeiss).

## Flow cytometry analysis

Colonic tissues (tumor and paired normal colonic mucosa) were recovered in a tissue storage solution (MACS Medium, Miltenyi Biotec) and further dissected for flow cytometry analyses. Briefly, tissue were minced into 1–2 mm<sup>3</sup> fragments at room temperature in RPMI 1640 medium (Life Technologies), and then transferred into a GentleMACS C tube (Miltenyi Biotec) for 2 rounds of nonenzymatic mechanical dissociation with a GentleMacs Dissociator (Program A.01, Miltenyi Biotec). Mucus and large debris were removed by filtration through a 40  $\mu\text{m}$  cell strainer (Dutscher). The suspension was centrifuged for 15 min at 600g at room temperature, and finally suspended

in RPMI 1640 before the ex vivo flow cytometry analyses. Peripheral blood mononuclear cells were isolated from peripheral blood of the patients using lymphocyte separation medium (Eurobio). Immediately after dissociation,  $2 \times 10^5$  cells were incubated in 100  $\mu$ L of brilliant stain buffer (BD Biosciences) containing appropriate concentrations of specific or isotype control antibodies for 30 min at 4 °C. Antibodies used are anti-human CD3-Brilliant Violet (BV) 421 (clone UCHT1), TCR  $\alpha\beta$ -BV510 (clone T10B9.1A-31), TCR  $\gamma\delta$ -Allophycocyanin (APC) (clone B1), CD8-BV650 (clone RPA-T8), CD8 $\alpha$ -Phycoerythrin (PE) (clone HIT8a), CD4-BV786 (clone L200), CD56-APC (clone B159), CD94-fluorescein isothiocyanate (FITC) (clone HP3D9), NKG2A-Alexa Fluor 700 (clone 131411), and NKG2C-PE (clone 134591). Dead cells were identified with the viability marker Zombie NIR (BioLegend). After washing in PBS 0.1% bovine serum albumin (BSA), stained cells were acquired in the viable cell gate on a Fortessa X-20 flow cytometer using BD Diva software (BD Biosciences) and further analyzed with FlowJo software.

### Generation of tumor-infiltrating CD8 T-cell lines and culture

Tumor-infiltrating lymphocytes from 10 colorectal cancer patients, 5 microsatellite stable (C9, C13, C81, C87, and C91 C), and 6 microsatellite instable (C62, C65, C95, C97 and C100) were obtained after culture of tumor fragments (approximately 1 mm<sup>3</sup>) during 3 weeks in RPMI 1640 medium supplemented with 8% human serum (Proleukin, Novartis), 2 mM L-glutamine, 100 U/mL penicillin, 0.1 mg/mL streptomycin, 0.1 mg/mL gentamycin (Sigma-Aldrich), and 150 U/mL of IL-2. After magnetic cell sorting using the Miltenyi microbeads cell isolation kit (positive selection), CD8<sup>+</sup> tumor-infiltrating lymphocytes were expanded by stimulation with PHA-L (Sigma-Aldrich, L4144) and 150 U/mL human rIL-2 in the presence of allogeneic irradiated feeder cells (peripheral blood mononuclear cells and B-EBV B cells) as previously described [20]. For functional tests, pure CD94/NKG2A-negative and -positive CD8<sup>+</sup> tumor-infiltrating lymphocytes from the C65 patient were generated by cell sorting using the BD FACSAria III cell sorter (BD Biosciences). Tumor infiltrating lymphocytes were stained with FITC-conjugated anti-CD94 mAb (Clone HD-3D9, BD Biosciences, 555888) and PE-conjugated anti-NKG2A mAb (Clone 131411, R&D, FAB1059P) for 30 min at 4 °C in PBS 0.1% BSA and then washed two times in PBS 0.1% BSA (Sigma-Aldrich, A9576) before cell sorting. To ensure that CD94/NKG2A positive phenotype does not result from doublets, these latter were excluded using FSC-A/FSC-H and SSC-A/SSC-H dot plots. The purity of each sorted T-cell population was checked after cell sorting by flow cytometry.

Twenty-four hours later, sorted cells were amplified in culture as described above.

### Redirected cytolytic activity

Murine mastocytoma Fc $\gamma$ R P815 cells ( $3 \times 10^3$  cells) were labeled with <sup>51</sup>Cr and then were co-cultured with  $3 \times 10^4$  effector sorted CD8<sup>+</sup> tumor-infiltrating lymphocytes expressing or not CD94/NKG2A from C65 patient in the presence of anti-CD3 Ab (clone OKT3) used at different concentrations. Anti CD3-mediated redirected lysis of P815 cells was modulated by the presence of 5  $\mu$ g/ml of anti-CD94 mAb (clone HP-3B1) or mouse IgG2a isotypic control. After 4 h, radioactive content was measured and percentage of specific lysis was calculated according to the following formula: [(experimental release – spontaneous release)/(maximum release – spontaneous release)]  $\times$  100. Maximum and spontaneous releases were determined by, adding 0.1% Triton X-100 or medium respectively to <sup>51</sup>Cr-labeled target cells in the absence of T cells.

### Statistics

The relation between the different immunological biomarkers (CD8, CD94, NKp46, and HLA-E/ $\beta$ 2m) and clinicopathological features were assessed using chi-square test or Fisher's exact test for qualitative variables and a non-parametric Mann–Whitney test for continuous variables. All statistical analyses were performed using GraphPad Prism 7 software. Five-year overall survival was measured from date of surgery to the date of death related to colorectal cancer, or latest follow-up. Disease-free survival was measured from the date of surgery to the date of disease relapse, or metastases, and, for stage IV patients, from the date of surgery to the date of new relapse or metastases. The prognostic influence of the different parameters (stage, age, CD8, CD94, and microsatellite status) was evaluated using the Kaplan–Meier method and compared by the log-rank test. Cox regression model was used to perform univariate analysis, and multivariate analysis was performed using a Cox proportional hazards regression model including all factors with  $p < 0.1$ . For phenotypic and functional analysis (cohort 2), Mann–Whitney test, Kruskal–Wallis test or Wilcoxon signed rank test has been used. A  $p$  value of less than 0.05 was considered as statistically significant.

## Results

### Patient population

Detailed clinicopathological and molecular characteristics of the two cohorts of patients are summarized in Table 1.

**Table 1** Clinicopathological and molecular features of CRC patients

	Cohort 1, <i>n</i> = 234			Cohort 1 (patients under 75 years of age) <i>n</i> = 130			Cohort 2, <i>n</i> = 27	
	MSI	MSS	<i>p</i> Value	MSI	MSS	<i>p</i> Value	MSI	MSS
	<i>N</i> = 47 <i>N</i> (%)	<i>N</i> = 187 <i>N</i> (%)		<i>N</i> = 21 <i>N</i> (%)	<i>N</i> = 109 <i>N</i> (%)		<i>N</i> = 11 <i>N</i> (%)	<i>N</i> = 16 <i>N</i> (%)
Age: mean (range)	72.2 (23–89)	69.7 (36–94)		62.9 (23–74)	61.2 (36–74)		77.4 (63–88)	72.8 (51–90)
<i>Gender</i>								
Men	13 (27.6)	122 (65.3)		7 (33.3)	68 (62.4)		2 (18)	11 (69)
Women	34 (72.3)	65 (34.7)	3.10 <sup>-6</sup>	14 (66.7)	41 (37.6)	0.01	9 (82)	5 (31)
<i>Tumor location</i>								
Right	44 (91.6)	86 (46)	2.10 <sup>-8</sup>	20 (95.3)	40 (36.7)	8.10 <sup>-7</sup>	10	7
Left	2 (4.2)	92 (49.2)		1 (4.7)	63 (57.8)		0	9
Transverse	2 (4.2)	6 (3.2)		0	3 (2.7)		1	0
Rectum	0	3 (1.6)		0	3 (2.75)		0	1
<i>Histological subtypes</i>								
Adenocarcinoma not otherwise specified (NOS)	27 (56.2)	158 (84.5)	4.10 <sup>-5</sup>	14 (66.6)	90 (82.5)	0.03	8	14
Mucinous adenocarcinoma	12 (25.5)	21 (14.4)	0.01	6 (28.6)	12 (9)	0.03	2	1
Medullary carcinoma	4 (8.3)	3 (1.6)	0.03	1 (4.8)	2 (1.5)	0.4	0	0
Mixed carcinoma	2 (4.1)	1 (0.5)		0	1 (0.7)		0	0
Signet ring cell carcinoma	1 (2)	1 (0.5)		0	1 (0.7)		0	0
Poorly differentiated carcinoma	1 (2)	2 (0.6)		0	2 (1.5)		1	0
Serrated carcinoma	0	1 (0.5)		0	1 (0.7)		0	1
<i>pT classification</i>								
pT0	0	2 (1)		0	2 (1.8)		0	0
pT1	0	10 (5.3)		0	6 (5.5)		1	1
pT2	1 (2)	13 (7)		1 (4.7)	6 (5.5)		1	4
pT3	30 (63.8)	122 (65.2)		14 (66.6)	70 (64.2)		6	8
pT4	16 (34)	40 (21.4)	0.02	6 (28.5)	25 (23)	0.4	3	3
<i>pN classification</i>								
Not precised	3	7		0	3			
pN0	21 (47.7)	74 (41.2)		11 (52.4)	52 (49)		7	10
pN1–N2	23 (52.3)	106 (58.8)		10 (47.6)	54 (51)		4	6
<i>UICC Stage</i>								
0	0	2 (1)		0	1 (0.9)		0	0
I	1 (2)	16 (8.5)		1 (4.7)	6 (5.5)		2	5
II	22 (46.8)	61 (32.6)		10 (47.6)	28 (25.7)		5	5
III	18 (38.3)	52 (27.8)		7 (33)	36 (33)		3	4
IV	6 (12.7)	56 (30)	0.02	3 (14.2)	39 (35.7)	0.04	1	2
M1a	2 (33.3)	35 (62.5)		2 (66.7)	28 (71.8)			
M1b	0	1 (1.8)		1 (33.3)	1 (2.6)			
M1c	4 (66.7)	17 (30.3)		0	8 (20.5)		1/1 (100)	2/2 (100)
Unknown	0	3 (5.4)		0	2 (5.1)			
<i>Mutational profile</i>								
<i>BRAF</i>	13/35 (37)	9/100 (9)	0.003	1/15 (6)	5/62 (8)		4/6	0
<i>RAS</i>	4/35 (11.5)	35/100 (35)	0.01	2/15 (13)	14/62 (22.5)		2/6	2/4
<i>WT</i>	18/35 (47.5)	56/100 (56)		12/15 (80)	43/62 (69)		2/6	2/4

WT wild type, MSS microsatellite stable, MSI microsatellite instable

Among the retrospective cohort 1 of 234 colorectal cancers, 47 were microsatellite instable (20%) and 187 were microsatellite stable (80%). The mutational profile of *BRAF* and *RAS* genes, performed as part of the diagnosis, was available for 135 patients (35 microsatellite instable and 100 microsatellite stable colorectal cancers). Among this cohort, patients under 75 years of age presented quite the same clinical and morphological characteristics. As expected, and in accordance with the literature, the clinicopathological features of this retrospective cohort according to the microsatellite status underlined the differences between microsatellite instable and microsatellite stable colorectal cancers with respect to female gender, right side tumor location, peculiar morphological features, such as mucinous or medullary subtypes, more advanced pT classification (pT3–T4 vs. pT0–T2), but lower distant metastasis and *BRAF* mutation in microsatellite instable colorectal cancers.

### HLA-E/ $\beta$ 2m is preferentially overexpressed in microsatellite instable colorectal cancers

HLA-E/ $\beta$ 2m was overexpressed by tumor cells in 23% (54/234) of colorectal cancers (Fig. 1a). Four percent (9/234) of colorectal cancers overexpressed HLA-E by tumor cells but without any co-expression of  $\beta$ 2m, and for this reason were not considered as HLA-E/ $\beta$ 2m<sup>+</sup>. HLA-E/ $\beta$ 2m-positive colorectal cancers were distributed within the different pTNM stages as follows: 0% stage 0 (0/2), 29.4% stage I (5/17), 16.9% stage II (14/83), 31.4% stage III (22/70), and 21.0% stage IV (13/62). Taking into account the different clinical and biological characteristics recently reported between right-sided and left-sided colorectal cancers [21], we addressed the relation between HLA-E/ $\beta$ 2m overexpression and tumor location and found that HLA-E/ $\beta$ 2m was preferentially overexpressed in right-sided (28.7%, 37/129) compared with left-sided colorectal

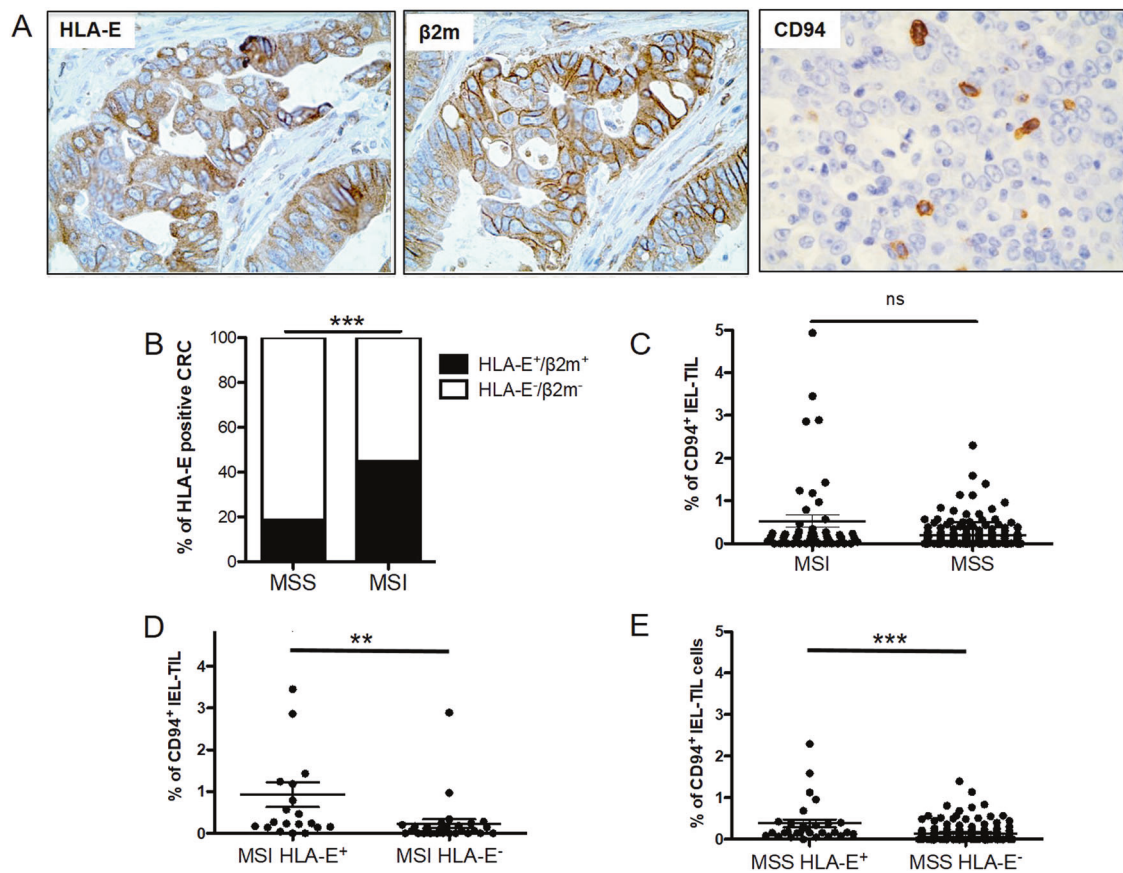


**Fig. 1** Overexpression of HLA-E/ $\beta$ 2m by tumor cells and density of CD94<sup>+</sup> intraepithelial tumor-infiltrating lymphocytes (IEL-TIL) depending on the microsatellite status of colorectal cancer (CRC). **a** Representative cases of a colorectal adenocarcinoma NOS overexpressing both HLA-E and  $\beta$ 2m by tumor cells and of a microsatellite instable medullary carcinoma infiltrated by a high number of CD94<sup>+</sup> intraepithelial tumor-infiltrating lymphocytes assessed by

immunohistochemistry ( $\times 400$ ). **b** Frequency of HLA-E/ $\beta$ 2m-positive colorectal adenocarcinoma depending on the microsatellite status. **c** Density of CD94<sup>+</sup> intraepithelial tumor-infiltrating lymphocytes according to the microsatellite status. **d**, **e** Density of CD94<sup>+</sup> intraepithelial tumor-infiltrating lymphocytes in microsatellite instable (MSI) (**c**) or microsatellite stable (MSS) (**d**) colorectal cancers (CRC) in relation with HLA-E/ $\beta$ 2m overexpression

cancers (14.9%, 14/94) ( $X^2$  test;  $p = 0.01$ ). The same trend was observed in colorectal cancer patients under 75 years of age (19.7% of HLA-E/ $\beta$ 2m positive right-side colorectal cancers vs. 15.8% among left-side colorectal cancers). Regarding the microsatellite status, HLA-E/ $\beta$ 2m was preferentially overexpressed in microsatellite instable (21/47; 44.7%) than in microsatellite stable colorectal cancers (35/187; 18.7%) ( $X^2$  test;  $p = 0.0002$ ) (Fig. 1b). The similar trend was observed in patients under 75 years of age (7/21; 33% in microsatellite instable colorectal cancers and 21/109; 19.2% in microsatellite stable colorectal cancers). However, no relation was observed between the mutational *BRAF/RAS* status and HLA-E/ $\beta$ 2m expression profile. Indeed, among HLA-E/ $\beta$ 2m<sup>+</sup> colorectal cancers, 49% (20/41) were mutated ( $n = 12$ , 31% *RAS* and  $n = 8$ , 38% *BRAF*) while 51% (21/41) were wild type.

### The density of intraepithelial tumor-infiltrating lymphocytes expressing the specific HLA-E/ $\beta$ 2m receptor—CD94/NKG2—is higher in colorectal cancers overexpressing HLA-E/ $\beta$ 2m

As CD94/NKG2 receptors are known to be specific for HLA-E/ $\beta$ 2m, we next searched for the presence of intraepithelial tumor-infiltrating lymphocytes in close contact with tumor cells expressing these receptors by immunohistochemistry. In paired normal colonic mucosa, we detected only scarce CD94<sup>+</sup> intraepithelial lymphocytes (0–0.0015%). By contrast, in colorectal cancers, we identified a higher number of CD94<sup>+</sup> intraepithelial tumor-infiltrating lymphocytes and their density was slightly higher in microsatellite instable (0.53%  $\pm$  0.15) than in microsatellite stable colorectal cancers (0.19%  $\pm$  0.02) ( $p = 0.0528$ ) (Fig. 1a–c). More interestingly, when considering the relation with HLA-E/ $\beta$ 2m overexpression by tumor cells, the density of CD94<sup>+</sup> intraepithelial tumor-infiltrating lymphocytes was significantly higher in HLA-E/ $\beta$ 2m<sup>+</sup> colorectal cancers compared with HLA-E/ $\beta$ 2m<sup>−</sup> colorectal cancers, either in microsatellite instable colorectal cancers (0.93%  $\pm$  0.30 in microsatellite instable HLA-E<sup>+</sup> vs. 0.23%  $\pm$  0.11 in microsatellite instable HLA-E<sup>−</sup>) ( $p = 0.0025$ ) and in microsatellite stable colorectal cancers (0.39%  $\pm$  0.10 in microsatellite stable HLA-E<sup>+</sup> vs. 0.15%  $\pm$  0.02 in microsatellite stable HLA-E<sup>−</sup>) ( $p < 0.0001$ ) (Fig. 1d, e).

### CD94<sup>+</sup> tumor-infiltrating lymphocytes predominantly co-express the NKG2A inhibitory chain and mainly correspond to CD8<sup>+</sup> $\alpha\beta$ tumor-infiltrating lymphocytes

As CD94 is known to be preferentially expressed by NK cells, but also by a subset of CD8<sup>+</sup> T lymphocytes [15], we assessed the density of both intraepithelial NK cells,

identified by the expression of the natural cytotoxicity receptor NKp46, and CD8<sup>+</sup> intraepithelial tumor-infiltrating lymphocytes by immunohistochemistry. Only 3% of colorectal cancers contained NKp46<sup>+</sup> intraepithelial NK cells, and their density was very low (mean 0.03%  $\pm$  0.01). The majority of colorectal cancers containing NKp46<sup>+</sup> intraepithelial NK cells were microsatellite instable (10.6% vs. 2.7% in microsatellite stable colorectal cancers) and their density was significantly higher in microsatellite instable (mean 0.09%  $\pm$  0.05) than in microsatellite stable colorectal cancers (0.01%  $\pm$  0.01) ( $p = 0.021$ ) (Fig. 2a–c). At the opposite, CD8<sup>+</sup> intraepithelial tumor-infiltrating lymphocytes were significantly more numerous than NKp46<sup>+</sup> intraepithelial tumor-infiltrating lymphocytes, also higher in microsatellite instable colorectal cancers, especially in medullary carcinomas, compared with microsatellite stable colorectal cancers (4.0%  $\pm$  0.77 vs. 1.2%  $\pm$  0.12;  $p < 0.0001$ ) (Fig. 2b, d).

To deepen these in situ analyses, especially to determine more precisely the phenotype of CD94<sup>+</sup> tumor-infiltrating lymphocytes, we performed ex vivo phenotype analyses of NK and T cells by flow cytometry on fresh resected samples of 17 colorectal cancers of the cohort 2 included prospectively. To facilitate these analyses, we enriched the prospective cohort 2 in microsatellite instable colorectal cancers ( $n = 11$ ), as microsatellite instable colorectal cancers were enriched in CD94<sup>+</sup> tumor-infiltrating lymphocytes. The phenotype of CD94<sup>+</sup> tumor-infiltrating lymphocytes was compared with that of lymphocytes and NK cells of paired normal colonic mucosa ( $n = 15$ ) and peripheral blood mononuclear cell samples ( $n = 8$ ). Flow cytometry gating strategy is depicted in Additional File 1 based on a representative case of tumor-infiltrating lymphocytes (C103). Flow cytometry analyses confirmed the scarcity of NK cells, as defined by CD3<sup>−</sup>CD16<sup>+/−</sup>CD56<sup>+</sup> lymphoid cells, in colorectal cancers, but also in healthy mucosa (4.3%  $\pm$  1.0 and 2.8%  $\pm$  0.5, respectively) compared with peripheral blood (28.1%  $\pm$  6.3). Furthermore, the proportion of T cells (CD3<sup>+</sup> lymphoid cells) was slightly higher in colorectal cancers than in paired healthy mucosa (35.0%  $\pm$  5.5 and 17.8%  $\pm$  3.5;  $p = 0.054$ ) (Fig. 3a). In addition, and as expected, the frequency of tumor-infiltrating T cells was higher, even not statistically significant, in microsatellite instable than in microsatellite stable colorectal cancers (49.3%  $\pm$  9.5 vs. 27.2%  $\pm$  5.7;  $p = 0.097$ ) (Fig. 3b). These cells mostly corresponded to  $\alpha\beta$  T cells (up to 90%),  $\alpha\beta$  T cells representing only 4.7%  $\pm$  1.4 in microsatellite instable and 2.3%  $\pm$  1.1 in microsatellite stable colorectal cancers (Fig. 3c). Furthermore, among these T cells, the proportion of CD8<sup>+</sup> T cells was significantly increased in microsatellite instable colorectal cancers compared with microsatellite stable colorectal cancers (40.6%  $\pm$  4.2 vs. 24.9%  $\pm$  3.5;  $p = 0.031$ ) (Fig. 3d).

**Fig. 2** Correlation between the density of Nkp46<sup>+</sup> or CD8<sup>+</sup> intraepithelial tumor-infiltrating lymphocytes (IEL-TIL) and the microsatellite status of colorectal cancers. **a, b** A representative case of microsatellite instable medullary carcinoma infiltrated by some rare Nkp46<sup>+</sup> cells (**a**, ×400) and a high number of CD8<sup>+</sup> intraepithelial tumor-infiltrating lymphocytes (**b**, ×200) assessed by immunohistochemistry. **c, d** Density of Nkp46<sup>+</sup> (**c**) and CD8<sup>+</sup> (**d**) intraepithelial tumor-infiltrating lymphocytes according to the microsatellite status (microsatellite stable (MSS) and microsatellite instable (MSI))

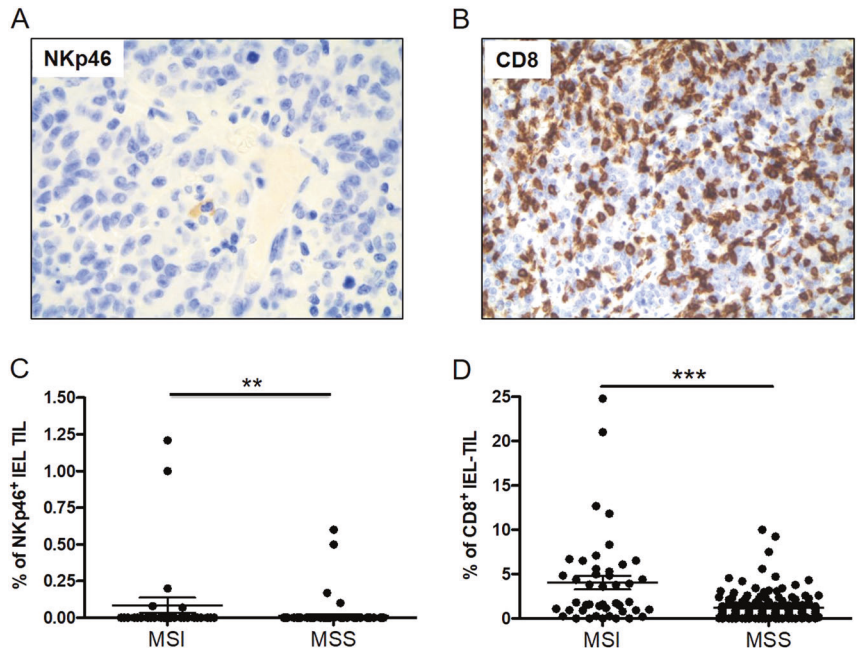
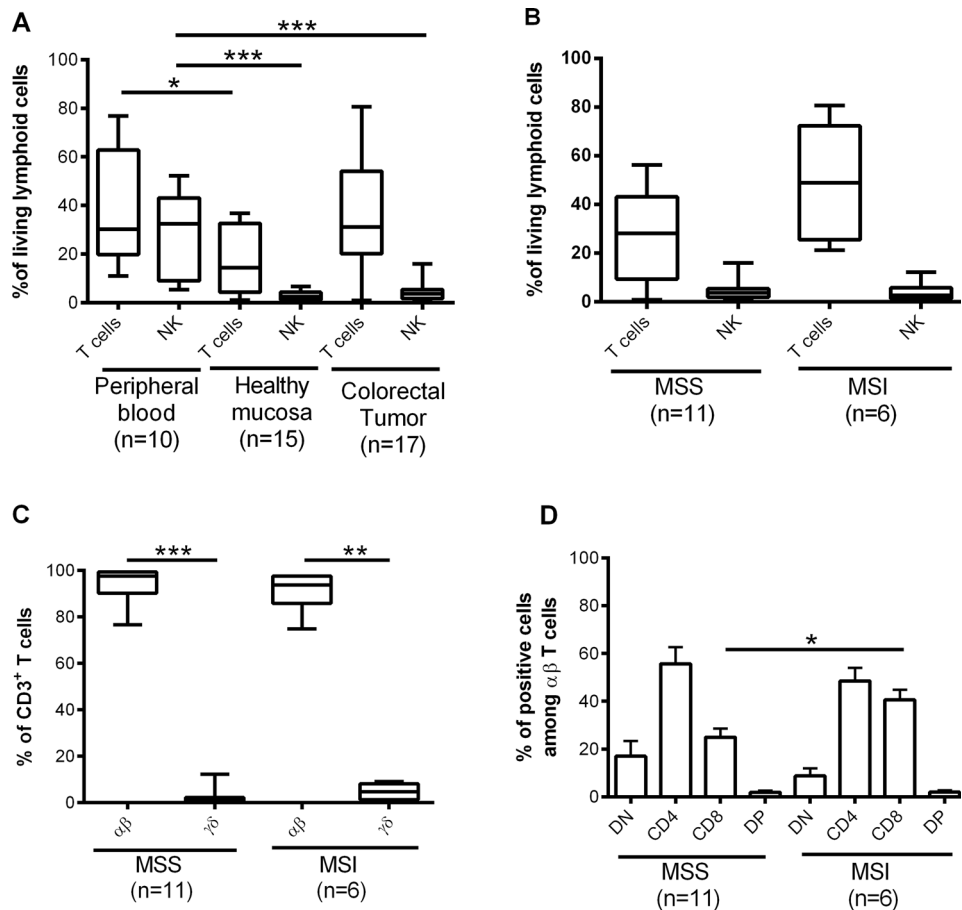


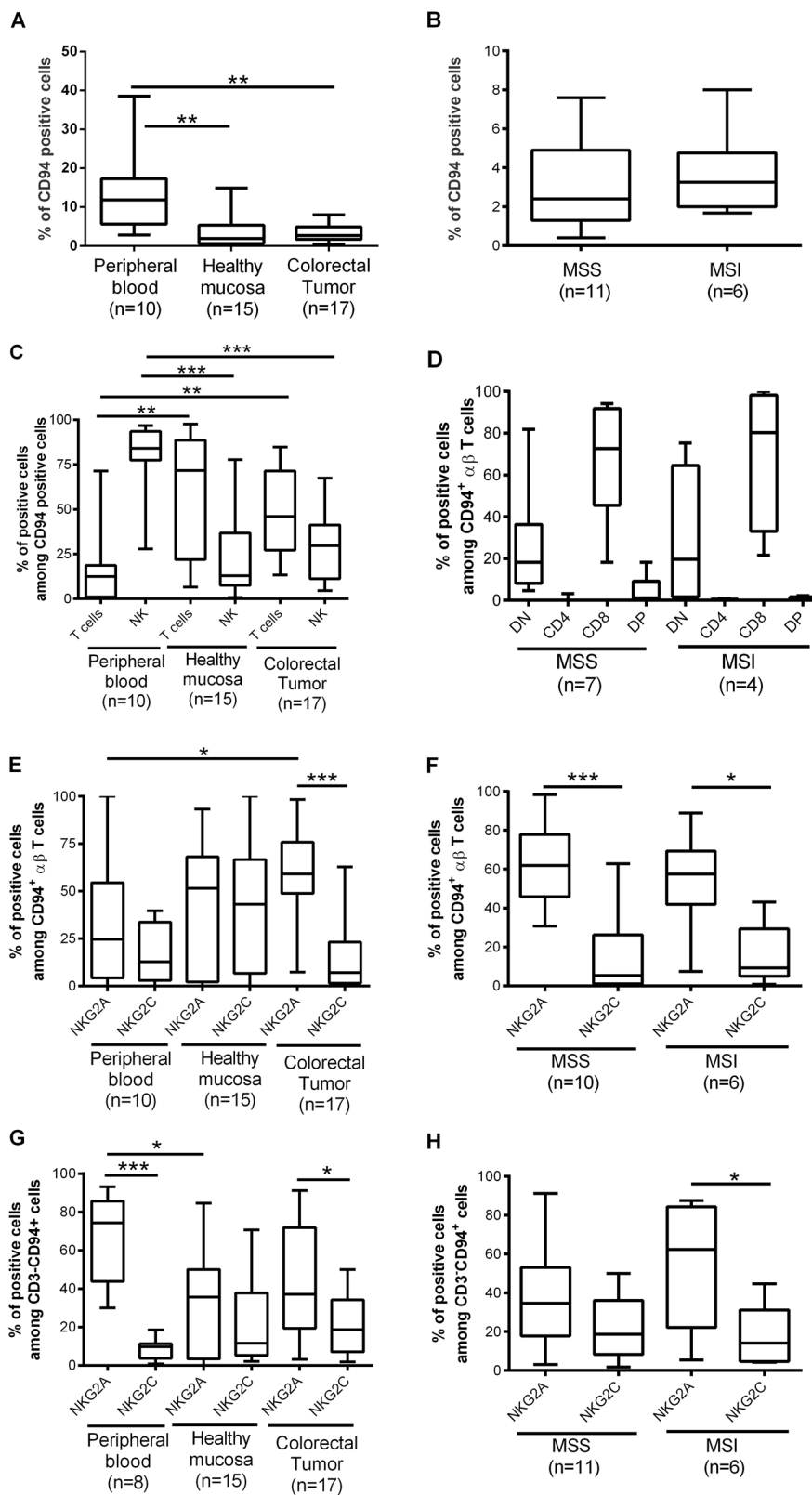
**Fig. 3** Frequency of NK and T cells in peripheral blood and in ex vivo dissociated healthy mucosa and colorectal tumor according to the microsatellite status. **a** Percentages of CD3<sup>+</sup> T cells and CD3<sup>-</sup>CD56<sup>+</sup> CD16<sup>+/−</sup> NK cells among living lymphoid cells in peripheral blood (*n* = 10), healthy mucosa (*n* = 15), and colorectal cancer (*n* = 17). **b** Proportion of T cells and NK cells in microsatellite stable (MSS) (*n* = 11) and microsatellite instable (MSI) (*n* = 6) colorectal cancers. **c** Proportion of αβ and γδ T cells among CD3<sup>+</sup> T cells in microsatellite stable and microsatellite instable colorectal cancers. **d** Distribution of CD3<sup>+</sup> T cells depending on CD4 and CD8 expression (simple positive CD4 and CD8 T cells, DP double positive T cells and DN double negative T cells) in colorectal cancers



Concerning the expression profile of CD94, the frequency of CD94<sup>+</sup> cells was significantly higher in peripheral blood (13.8% ± 4.0) than in paired tissues, healthy

colonic mucosa (4.5% ± 1.4; *p* = 0.007) or colorectal cancers (3.3% ± 0.6; *p* = 0.002) irrespective of the microsatellite status (Fig. 4a, b). As expected, in peripheral blood,

**Fig. 4** *Ex-vivo* expression of CD94, mostly associated with NKG2A, by CD8  $\alpha\beta$  T cells and NK cells among immune infiltrating cells in colorectal cancers. **a** Percentages of CD94<sup>high</sup> expressing cells among living lymphoid cells in peripheral blood ( $n = 10$ ), healthy mucosa ( $n = 15$ ), and colorectal cancer ( $n = 17$ ). **b** Percentages of CD94<sup>high</sup> expressing cells among living lymphoid cells in microsatellite stable (MSS) ( $n = 11$ ) and microsatellite instable (MSI) ( $n = 6$ ) colorectal cancers. **c** Percentages of T cells and NK cells among CD94<sup>+</sup> cells in peripheral blood, healthy mucosa and colorectal tumor. **d** Repartition of CD94<sup>+</sup>  $\alpha\beta$  T cells depending on CD4 and CD8 expression (simple positive CD4 and CD8 T cells, DP double positive T cells and DN double negative T cells) in microsatellite stable and microsatellite instable colorectal cancers. **e, g** Expression of NKG2A and NKG2C by CD94<sup>+</sup>  $\alpha\beta$  T cells (**e**) or NK cells (**g**) in peripheral blood, healthy mucosa and colorectal cancer. **f, h** Expression of NKG2A and NKG2C by CD94<sup>+</sup>  $\alpha\beta$  T cells (**f**) or NK cells (**h**) in microsatellite stable and microsatellite instable colorectal cancers



CD94<sup>+</sup> cells mainly corresponded to NK cells (near 80%), while in colorectal cancers these CD94<sup>+</sup> cells are distributed among NK (30.2%  $\pm$  4.9) or T cells (49.2%  $\pm$  5.7)

(Fig. 4c). The CD94<sup>+</sup> T cells, which possess  $\alpha\beta$  TCR, predominantly corresponded to CD8<sup>+</sup> T cells in microsatellite stable and microsatellite instable CRC (67.4%  $\pm$

10.8 and 70.5% ± 17.8, respectively) expressing the CD8 αβ heterodimer (Fig. 4d and data not shown). CD94 expression by CD4<sup>+</sup> T cells was almost undetectable (<0.5%). Given the predominance of T cells over NK cells in colorectal cancers, CD94<sup>+</sup> tumor-infiltrating lymphocytes mainly corresponded to CD8 αβ T cells in microsatellite instable as well as in microsatellite stable colorectal cancers (Fig. 4c, d).

In order to determine more precisely which inhibitory (NKG2A) or activating (NKG2C) chain was co-expressed with CD94, we then assessed the expression profile of these two chains on CD94<sup>+</sup> T and NK cells. In peripheral blood, there was twofold more CD94/NKG2A<sup>+</sup> cells than CD94/NKG2C<sup>+</sup> cells (32.9% ± 11.9 vs. 17.6% ± 5.4;  $p = 0.260$ ) (Fig. 4e). Interestingly, while the proportion of CD94/NKG2A<sup>+</sup> αβ T cells and CD94/NKG2C<sup>+</sup> αβ T cells was quite similar in healthy colonic mucosa, the density of CD94/NKG2A<sup>+</sup> αβ tumor-infiltrating lymphocytes was significantly higher than the density of CD94/NKG2C<sup>+</sup> αβ tumor-infiltrating lymphocytes in colorectal cancers (59.3% ± 5.6 vs. 15.7% ± 4.9;  $p < 0.0001$ ), irrespective of the microsatellite status (Fig. 4e, f). Similarly, while the proportion of CD94/NKG2A<sup>+</sup> NK cells and CD94/NKG2C<sup>+</sup> NK cells was quite similar in healthy colonic mucosa, CD94<sup>+</sup> NK cells were mostly associated with the NKG2A inhibitory chain than with the NKG2C activating one in colorectal cancers (43.9% ± 7.2 vs. 19.9% ± 3.7) irrespective of the microsatellite status (Fig. 4g, h).

Taking into account these flow cytometry data that do not distinguish intraepithelial tumor-infiltrating lymphocytes from tumor-infiltrating lymphocytes of the stroma, we used double immunofluorescence on frozen sections (two colorectal cancers, one microsatellite instable, and one microsatellite stable selected for their high numbers of CD94<sup>+</sup> intraepithelial tumor infiltrating lymphocytes) to verify the co-expression of NKG2A by CD94<sup>+</sup> intraepithelial tumor-infiltrating lymphocytes. Interestingly, co-expression of NKG2A and CD94 was observed on some intraepithelial tumor-infiltrating lymphocytes on both microsatellite instable and microsatellite stable colorectal cancers (Additional File 2).

### The engagement of CD94/NKG2A inhibits the TCR-dependent lytic activity of CD8<sup>+</sup> tumor-infiltrating lymphocytes

In order to address the biological function of CD94/NKG2A receptor, we first derived polyclonal populations of tumor-infiltrating lymphocytes from 12 colorectal cancers of the cohort 2 (6 microsatellite instable and 6 microsatellite stable), then sorted CD8<sup>+</sup> T cells and analyzed the CD94/NKG2A expression profile by those CD8<sup>+</sup> T cells. Representative histograms of CD94 expression by 2 of these

CD8<sup>+</sup> TIL populations (C65 and C87) are shown in Fig. 5a. As shown in Fig. 5b, all TIL populations analyzed ( $n = 12$ ) contained CD94<sup>+</sup> cells with heterogeneous proportions ranging from 0.5% (C13) to 42% (C65) of them. In addition, CD94 was always co-expressed with the NKG2A inhibitory chain (data not shown). Interestingly, colorectal cancers featuring the highest percentage of CD94/NKG2A<sup>+</sup> tumor-infiltrating lymphocytes among CD8<sup>+</sup> tumor-infiltrating lymphocytes assessed by flow cytometry corresponded consistently to those with the highest density of CD94<sup>+</sup> intraepithelial tumor-infiltrating lymphocytes assessed by immunohistochemistry, suggesting that our culture protocol does not influence CD94 membrane expression (data not shown).

For functional analysis, we separated by fluorescence-activated cell sorting CD94/NKG2A<sup>+</sup> from CD94/NKG2A<sup>-</sup> cells among CD8<sup>+</sup> tumor-infiltrating lymphocytes from the colorectal cancer containing the highest proportion of CD94<sup>+</sup> tumor-infiltrating lymphocytes (C65) (Fig. 5c). As we failed to establish an autologous tumor cell line derived from these colorectal cancers, we used the murine FcR<sup>+</sup> P815 cell line as target cells to analyze by a redirected lysis assay the ability of an anti-CD94 mAb to modulate TCR-dependent lysis of CD8<sup>+</sup> tumor-infiltrating lymphocytes. As shown in Fig. 5d, anti-CD3 mAb-induced lysis was similar between CD94/NKG2A<sup>+</sup> and CD94/NKG2A<sup>-</sup> CD8<sup>+</sup> TIL subpopulations. However, this CD3-induced lytic activity decreased significantly in the CD94/NKG2A<sup>+</sup> subpopulation ( $p = 0.001$ ) when adding the cross-linking anti-CD94 mAb, compared with the IgG2a isotype control. By contrast, the cross-linking anti-CD94 mAb did not modify the CD3-induced lysis of the CD94/NKG2A<sup>-</sup> subpopulation ( $p = 0.092$ ). These data demonstrate the functional activity of this inhibitory receptor expressed by tumor-infiltrating lymphocytes from colorectal cancers and strongly suggest that the TCR-dependent lytic activity of CD8 CD94/NKG2A<sup>+</sup> tumor-infiltrating lymphocytes can be inhibited in vivo through engagement of CD94/NKG2A receptors by HLA-E/β2m-positive tumor cells.

### The density of CD94/NKG2<sup>+</sup> intraepithelial tumor-infiltrating lymphocytes represents an independent predictor of poor overall survival in colorectal cancer patients under 75 years of age

Taking into account all of these phenotypic and biological data, demonstrating (i) the predominance of CD94/NKG2A<sup>+</sup> over CD94/NKG2C<sup>+</sup> CD8<sup>+</sup> tumor-infiltrating lymphocytes present in close contact with tumor cells, and (ii) the inhibitory function of the CD94/NKG2A receptor, we then addressed the prognostic relevance of CD94<sup>+</sup> intraepithelial tumor-infiltrating lymphocytes. At the end of the follow-up period (censored at 5 years), 39 patients (30%) had died. The results of survival analysis, taking into account the stage, the

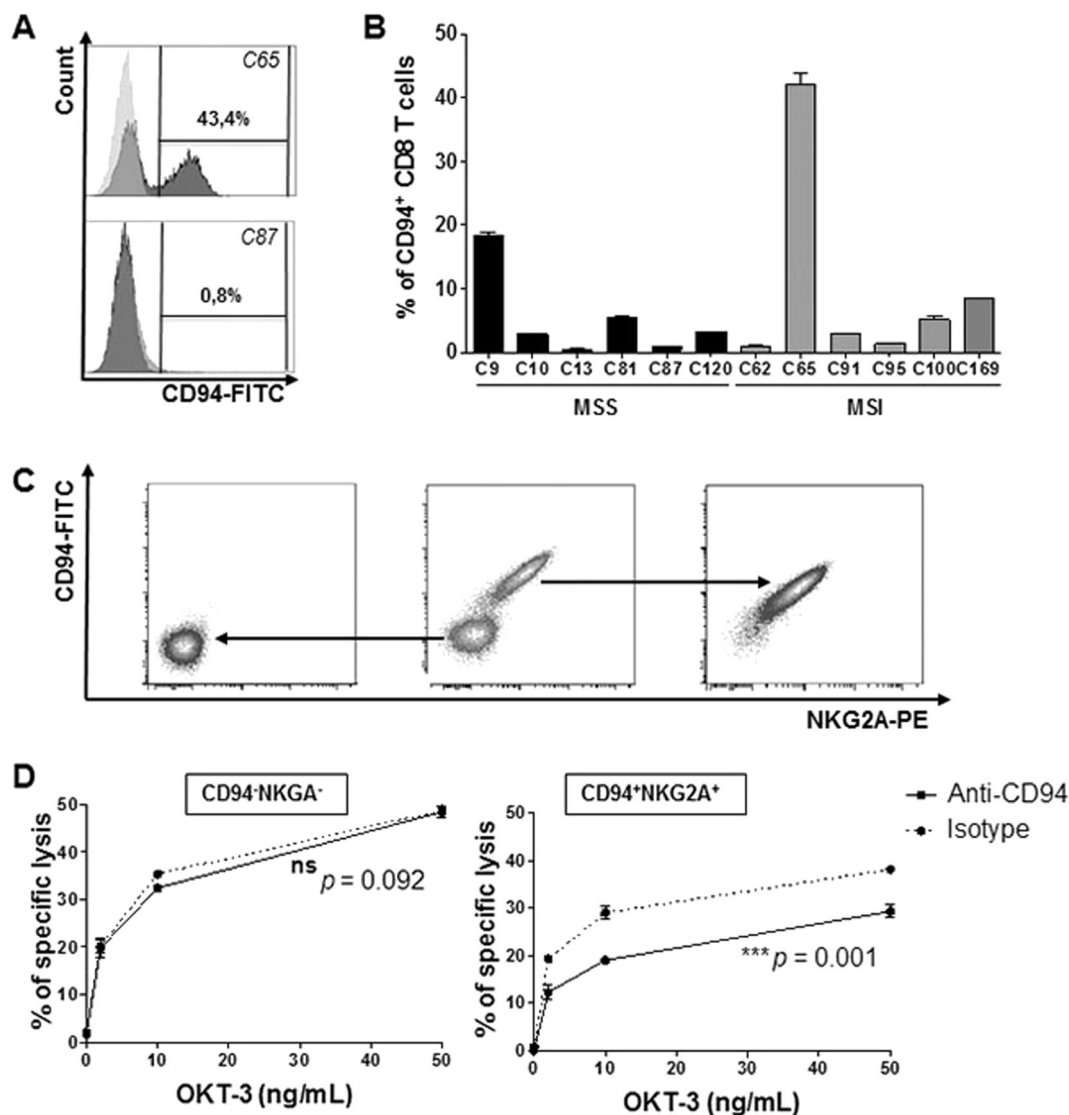


**Fig. 5** Modulation of CD8<sup>+</sup> tumor-infiltrating lymphocytes reactivity through CD94/NKG2A engagement. **a, b** Surface expression of CD94 by CD8<sup>+</sup> tumor-infiltrating lymphocytes isolated from colorectal cancers. Representative histograms of CD94 expression by two populations (C65 and C87) (**a**). Frequency of CD94<sup>+</sup> cells among CD8<sup>+</sup> tumor infiltrating lymphocytes derived from 12 colorectal cancers (6 microsatellite stable (MSS) and 6 microsatellite unstable (MSI)) (**b**). **c** Flow cytometry cell sorting of CD94/NKG2A negative and positive CD8<sup>+</sup> tumor infiltrating lymphocytes derived from colorectal cancer C65 and verification of the purity of sorted cells. **d** Cross-linking of CD94/NKG2A<sup>+</sup> CD8<sup>+</sup> tumor-infiltrating lymphocytes (but not CD94/NKG2A<sup>-</sup> cells) by anti-CD94 mAb inhibits the

anti-CD3-mediated cytolytic activity against FcγR<sup>+</sup> target cells. <sup>51</sup>Cr-labeled P815 cells were preincubated with the indicated concentration of anti-CD3 antibody in the presence or not of the indicated anti-CD94 mAb or mouse IgG2a isotypic control for 1 h. Then, CD94/NKG2A positive and negative-sorted CD8<sup>+</sup> tumor-infiltrating lymphocyte subpopulations from patient C65 were added for 4 h at an E:T of 10:1. Redirected cytotoxic activity was assessed through measurement of <sup>51</sup>Cr release in the supernatants. Percentages of specific lysis are indicated. Means and standard deviations of triplicate wells are shown for one representative experiment out of four performed. A Wilcoxon signed-rank test was used to compare results with or without addition of anti-CD94 mAb

microsatellite status, and densities of CD8<sup>+</sup> and CD94<sup>+</sup> intraepithelial tumor-infiltrating lymphocytes, are summarized in Table 2. As expected, in univariate analysis, patients with microsatellite unstable colorectal cancer had a longer 5-year disease-free survival and overall survival than patients with microsatellite stable colorectal cancer. Regardless of the microsatellite status, patients with a high density of CD8<sup>+</sup>

intraepithelial tumor-infiltrating lymphocytes had a longer 5-year disease-free survival and overall survival, but the differences were not statistically significant. By contrast, as a continuous parameter, density of CD94<sup>+</sup> intraepithelial tumor-infiltrating lymphocytes showed a strong prognostic relevance for overall survival, and in multivariate analysis, the expression of this HLA-E-engaged receptor was an

**Table 2** Univariate and multivariate Cox analyses for OS in the cohort of CRC patients under 75 years of age ( $n = 130$ )

	Overall survival (OS)			
	Univariate Cox analysis		Multivariate Cox analysis	
	Hazard ratio (95% CI)	<i>p</i> Value	Hazard ratio (95% CI)	<i>p</i> Value
Stage III/IV vs. I/II	5.08 (1.8–14.3)	<b>0.002</b>	4.55 (1.58–13.1)	<b>0.005</b>
CD8 (continuous variable)	0.75 (0.55–1.03)	0.07	0.78 (0.57–1.07)	0.12
CD94 (continuous variable)	1.46 (0.96–2.2)	0.07	1.67 (1.03–2.71)	<b>0.03</b>
MSI vs. MSS	0.79 (0.33–1.9)	0.6	0.82 (0.32–2.15)	0.69
<i>Disease free survival (DFS)</i>	Univariate Cox analysis		Multivariate Cox analysis	
	Hazard ratio (95% CI)	<i>p</i> Value	Hazard ratio (95% CI)	<i>p</i> Value
Stage III/IV vs. I/II	4.91 [2.09–11.5]	<b>0.0003</b>	1.63 [1.63–9.41]	<b>0.0023</b>
CD8 (continuous variable)	0.77 [0.60–1.00]	0.052	0.79 [0.60–1.05]	0.10
CD94 (continuous variable)	1.30 [0.85–1.98]	0.22	1.48 [0.92–2.39]	0.10
MSI vs. MSS	0.66 [0.30–1.46]	0.30	0.85 [0.36–2.00]	0.71

*CI* confidence interval

independent poor prognostic factor, as well as the stage. If one excluded the stage from the multivariate analysis, the density of CD8<sup>+</sup> intraepithelial tumor-infiltrating lymphocytes became an independent favorable prognostic factor in terms of both overall survival (HR = 0.70, 95% CI: [0.50–0.97],  $p = 0.03$ ) and disease-free survival (HR = 0.72, 95% CI: [0.54–0.97],  $p = 0.03$ ).

Since the density of CD94<sup>+</sup> intraepithelial tumor-infiltrating lymphocytes as a continuous parameter was an independent poor prognostic factor, we searched for the best cut-point for patient stratification. Strategy has consisted in determining the appropriateness of a cut-point model (graphical diagnostic plot) and, if relevant, estimate this cut point based on the method proposed by Contal and O'Quigley (macro SAS % findcut) [22]. By this method, we found a cut-point of 0.37% of CD94<sup>+</sup> intraepithelial tumor-infiltrating lymphocytes. After dichotomization, a density of CD94<sup>+</sup> intraepithelial tumor-infiltrating lymphocytes > 0.37% seemed to confer a worse 5-year overall survival in Kaplan–Meier survival analysis but the survival time difference was not statistically significant ( $p = 0.12$ ).

## Discussion

A better understanding of the balance between immune control and immune escape in tumor development/progression is crucial for the identification of new immunotherapeutic targets, besides programmed cell death 1 (PD1)/programmed cell death 1 ligand (PDL1) axis, and for the design of new immunotherapies to reinvigorate the anti-tumor immune response in colorectal cancer. Our comprehensive and multiparametric analysis highlights four major points with a potential clinical relevance: (i) HLA-E/β2m is

preferentially overexpressed by tumor cells in microsatellite instable compared with microsatellite stable colorectal cancers, (ii) colorectal cancers overexpressing HLA-E/β2m carry the highest density of CD94<sup>+</sup> intraepithelial tumor-infiltrating lymphocytes irrespective of the microsatellite status, (iii) these CD94<sup>+</sup> tumor-infiltrating lymphocytes correspond mainly to CD8<sup>+</sup> αβ T cells that co-express a functional NKG2A inhibitory chain, and finally (iiii) a high density of CD94<sup>+</sup> intraepithelial tumor-infiltrating lymphocytes is an independent poor prognostic factor in colorectal cancers.

The current study confirms on a larger cohort of colorectal cancers patients the overexpression of HLA-E/β2m by tumor cells of primary tumors in approximately 20% of colorectal cancers, with respect to the results of our more restricted previous study [16], and in line with a recent study [23]. Most interestingly, our results herein reveal a preferential overexpression of this nonclassical MHC class I molecule in right-sided and microsatellite instable colorectal cancers (45%) compared with left-sided and microsatellite stable colorectal cancers (18%), irrespective of their *RAS* or *BRAF* mutational status. Only one study by Zeestraten et al. [24] addressed the relation between HLA-E expression and microsatellite status in colorectal cancers, without identifying significant association. This discordant result could be explained by a higher percentage of HLA-E<sup>+</sup> tumors identified in their study (76%) than in our study (24%). This variation could be accounted for by a different HLA-E scoring method. Indeed, we only considered the aberrant strong overexpression of HLA-E by tumor cells compared with the absence or faint expression by paired normal epithelial cells. Moreover, the authors did not assess the β2m co-expression besides HLA-E, this invariant chain being mandatory for the stability and the functionality of this heterodimer [14]. In our study, 4% of HLA-E<sup>+</sup> colorectal

cancers have lost the expression of  $\beta 2m$  and thus were not considered overexpressing HLA-E.

One of the key findings of this study is the demonstration of the strong and significant association between HLA-E/ $\beta 2m$  overexpression by tumor cells and a high density of CD94<sup>+</sup> intraepithelial tumor-infiltrating lymphocytes intercalated between tumor cells, often co-expressing an inhibitory NKG2A chain, irrespective of the microsatellite status. The presence of NKG2A<sup>+</sup> tumor-infiltrating lymphocytes has been reported in cervical and ovarian cancers [25–27], and more recently in HLA-E<sup>+</sup> colorectal cancers [23]. The fact that a subgroup of microsatellite stable colorectal cancers (19%) overexpress HLA-E and contain inhibited CD94/NKG2A<sup>+</sup> tumor-infiltrating lymphocytes is a major finding as for the meantime, microsatellite stable colorectal cancers are excluded from the field of immunotherapies. Since this inhibitory receptor is mostly expressed on NK cells, we searched for the identification of NK cells both by immunohistochemistry and flow cytometry. In accordance with previous studies [23, 28], we only identified scarce NK cells both within tumor nests or in the stroma, compared with the high number of CD8<sup>+</sup> tumor-infiltrating  $\alpha\beta$  T lymphocytes ( $\approx 4\%$  vs. 35% of lymphoid cells, respectively). Most interestingly, about 3% of CD94<sup>+</sup> tumor-infiltrating lymphocytes (1/3 of NK cells and 2/3 of CD8<sup>+</sup>  $\alpha\beta$  T cells) co-expressed the NKG2A inhibitory chain. Taking into account the marked preponderance of CD8<sup>+</sup> tumor-infiltrating lymphocytes compared with NK cells in the tumor microenvironment, we can clearly consider that the majority of CD94/NKG2A<sup>+</sup> tumor-infiltrating lymphocytes correspond to CD8<sup>+</sup>  $\alpha\beta$  T cells in colorectal cancers as previously reported in gynecological cancers [25, 29, 30]. Interestingly, while the expression of CD94/NKG2A<sup>+</sup> mostly characterized NK cells in the peripheral blood, in tumors CD94/NKG2A<sup>+</sup> cells mostly corresponded to CD8<sup>+</sup>  $\alpha\beta$  T cells. This profile has been recently observed in head and neck carcinomas, and could demarcate a tissue-resident CD8<sup>+</sup> T cell subtype as those CD94/NKG2A tumor-infiltrating lymphocytes frequently co-expressed CD103 [27].

Moreover, and most importantly, we demonstrated for the first time that this CD94/NKG2A receptor is functional as its engagement on CD8<sup>+</sup> tumor-infiltrating lymphocytes isolated from primary colorectal cancers leads to a significant decrease of their TCR-dependent lytic activity. These results are in accordance with those reported by van Hall and Gooden in gynecological cancers [25, 26]. Thus, our results strongly hypothesize that overexpression of HLA-E/ $\beta 2m$  by tumor cells hinder CD8<sup>+</sup> cytotoxic tumor-infiltrating lymphocytes (and to a lesser extent NK cells) expressing the inhibitory receptor CD94/NKG2A<sup>+</sup> and participate to an immune escape mechanism. Besides, in accordance with our phenotypic and functional results, this study is the first to highlight the unfavorable independent prognostic influence of CD94<sup>+</sup> intraepithelial tumor-infiltrating lymphocytes in terms of

overall survival in colorectal cancers. The same poor prognostic influence of CD94/NKG2A gene expression has been recently reported in head and neck squamous cell carcinomas [27].

Little is known about the regulation of HLA-E by tumor cells, especially in colorectal cancer. The preferential overexpression of HLA-E/ $\beta 2m$  in microsatellite instable, as well as in right-sided colorectal cancers we report here, could be related to the dense immune microenvironment associated with the majority of microsatellite instable colorectal cancers, located preferentially in right-sided colon. Indeed, recent transcriptomic analyses clearly demonstrated in microsatellite instable and in right-sided tumors an up-regulated immune signature including genes encoding the Th1/Tc1 immune response, such as *TBX21*, *CD8A*, and *IFN-gamma* (IFN- $\gamma$ )—the canonical Th1/Tc1 cytokine [7–9, 31]. In line with these data, we previously demonstrated, at the protein level, the highest density of tumor-infiltrating lymphocytes expressing the hallmark Th1 transcription factor—Tbet—, in microsatellite instable compared with microsatellite stable colorectal cancers, resulting in the highest basal concentration of IFN- $\gamma$  in the microsatellite instable tumor microenvironment [10]. As we and others demonstrated in vitro that IFN- $\gamma$  is able to induce the tumor-cell expression of HLA-E [12, 32], we can suggest that the preferential overexpression of HLA-E/ $\beta 2m$  by tumor cells in microsatellite instable and right-sided tumors is in relation with high levels of IFN- $\gamma$  in the microenvironment of those colorectal cancers. This association is in keeping with the adaptive immune resistance concept, explaining also the preferential expression of several inhibitory checkpoint ligands such as PDL1 in microsatellite instable colorectal cancers [9, 10]. Besides, we observed a frequent co-expression of HLA-E and PDL1 by tumor cells in microsatellite instable colorectal cancers, especially in medullary carcinomas (personal observation). Furthermore, and interestingly, the subgroup of microsatellite stable colorectal cancers overexpressing HLA-E/ $\beta 2m$  (19%) could correspond to a recently described subset of microsatellite stable colorectal cancers featuring an up-regulated intra-tumor adaptive immune gene expression, a high immunoscore [5], a high density of both Tbet<sup>+</sup> and PD1<sup>+</sup> tumor-infiltrating lymphocytes and high level of basal IFN- $\gamma$  in their microenvironment similar to microsatellite instable colorectal cancers [10].

From a clinical point of view, our results open an interesting alternative and promising immune checkpoint blockade in colorectal cancers since the inhibitory CD94/NKG2A receptor can be clinically targeted with the new developed humanized anti-NKG2A monoclonal antibody (monalizumab). Indeed, this monoclonal antibody is able in vitro to restore the anti-tumor cytotoxicity of NK cells and CD8<sup>+</sup> T cells against HLA-E<sup>+</sup> tumor-cell lines and presents additive effects with anti-PD1 or anti-EGFR antibodies [23]. Supporting these preclinical results, the phase I/II clinical trial of

combination of monalizumab and cetuximab led to a significant 30% objective response rate in advanced head and neck cancer patients [23]. As cetuximab plus chemotherapy is commonly used in *RAS* wild-type metastatic CRC patients with a preferential efficacy in left-sided colorectal cancers [33], the addition of anti-NKG2A antibody could represent a promising therapeutic option in the arsenal of immune checkpoint blockers, especially for microsatellite stable colorectal cancer patients that are not eligible to anti-PD1/anti-PDL1 antibodies. In microsatellite instable colorectal cancer patients who preferentially overexpressed HLA-E/β2m, the combination of monalizumab with anti-PD1/PDL1 antibodies could be considered to enhance objective response rate of PD1/PDL1 inhibitors as NKG2A is frequently co-expressed with PD1 on CD8<sup>+</sup> T cells, and this combination has demonstrated additive effects, at least on NK cell functions, in *in vitro* experiments [23].

In conclusion, our results strongly suggest that tumor cells in colorectal cancers, especially microsatellite instable but also a subgroup of microsatellite stable colorectal cancers, via aberrant overexpression of HLA-E/β2m, contribute to paralyze the antitumor immune attack by engaging the inhibitory CD94/NKG2A receptor on CD8<sup>+</sup> tumor-infiltrating lymphocytes, and to a lesser extent on NK cells. Thus, our results extend our knowledge of the immune contexture of colorectal cancer. Therefore, HLA-E/β2m-CD94/NKG2A axis represents a promising new inhibitory immune checkpoint in colorectal cancer that could be targeted with the recently generated humanized anti-NKG2A monoclonal antibody. Our pre-clinical data strongly suggest a potential therapeutic efficacy of this new anti-NKG2A antibody, at least in some colorectal cancers, and should be considered in future clinical trials for colorectal cancers. In this context, as for PDL1/PD1 immune checkpoint, HLA-E/β2m overexpression by tumor cells could be a potential predictive biomarker, easily assessable by immunohistochemistry on FFPE tumor tissues, to select colorectal cancer patients eligible for this promising NKG2A immune checkpoint inhibitor. Indeed, it seems obvious and crucial to verify the predictive role of HLA-E expression and to determine its appropriate predictive threshold in the future clinical trials using monalizumab in colorectal cancer patients.

**Acknowledgements** We acknowledge the technical and logistic support of Stéphanie Blandin from the Morphology facility (MicroPicell, SFR Bonamy, Nantes), the support of Cécile Girard from the Tumorothèque of Institut de Recherche contre le Cancer Nantes Atlantique, and the logistic support of the team of technicians from the Pathology Department of CHU Nantes. The authors also thank Sylvain Simon for flow cytometry cell sorting as well as Juliette Desfrancois-Noel and Nadège Marec from the CytoCell Cytometry Facility for expert technical assistance (Structure Fédérative de Recherche “Francois Bonamy”, Nantes). This work was supported by grants from the French “Direction de l’Hospitalization et l’Organisation des Soins” (DHOS) (PROG/09/03), Ligue contre le cancer Grand Ouest (Comités du Finistère, de Loire-Atlantique, Côtes d’Armor et Morbihan), DHU Oncogreff, CHU

Nantes (RC14-0416-1), Cancéropôle Grand Ouest (Réseau Immunothérapie—Amgen RC16-0212-1). This work was performed in the context of the LabEX IGO program supported by the National Research Agency via the investment of the future program ANR-11-LABX-0016-01. Juliette Eugene was the recipient of a fellowship from INSERM (Institut National de la Santé Et de la Recherche Médicale) and INCa (Institut National du Cancer) (Plan Cancer 2009–2013 AAC “Soutien pour la Formation à la Recherche Translationnelle en Cancérologie”) and Nicolas Jouand from the LabEX IGO.

## Compliance with ethical standards

**Conflict of interest** The authors declare that they have no conflict of interest.

**Publisher’s note:** Springer Nature remains neutral with regard to jurisdictional claims in published maps and institutional affiliations.

## References

- Pagès F, Berger A, Camus M, et al. Effector memory T cells, early metastasis, and survival in colorectal cancer. *N Eng J Med*. 2005;353:2654–66.
- Galon J. Type, density, and location of immune cells within human colorectal tumors predict clinical outcome. *Science*. 2006;313:1960–4.
- Reissfelder C, Stamova S, Gossmann C, et al. Tumor-specific cytotoxic T lymphocyte activity determines colorectal cancer patient prognosis. *J Clin Invest*. 2015;125:1364–1364.
- Pagès F, Mlecnik B, Marliot F, et al. International validation of the consensus immunoscore for the classification of colon cancer: a prognostic and accuracy study. *Lancet*. 2018;391:2128–39.
- Mlecnik B, Bindea G, Angell HK, et al. Integrative analyses of colorectal cancer show immunoscore is a stronger predictor of patient survival than microsatellite instability. *Immunity*. 2016;44:698–711.
- Banerjee A, Hands RE, Powar MP, et al. Microsatellite and chromosomal stable colorectal cancers demonstrate poor immunogenicity and early disease recurrence. *Colorectal Dis*. 2009;11:601–8.
- Guinney J, Dienstmann R, Wang X, et al. The consensus molecular subtypes of colorectal cancer. *Nat Med*. 2015;21:1350–6.
- Marisa L, de Reyniès A, Duval A, et al. Gene expression classification of colon cancer into molecular subtypes: characterization, validation, and prognostic value. *PLoS Med*. 2013;10:e1001453.
- Llosa NJ, Cruise M, Tam A, et al. The vigorous immune microenvironment of microsatellite instable colon cancer is balanced by multiple counter-inhibitory checkpoints. *Cancer Discov*. 2015;5:43–51.
- Ott E, Bilonda L, Dansette D, et al. The density of Tbet+ tumor-infiltrating T lymphocytes reflects an effective and druggable preexisting adaptive antitumor immune response in colorectal cancer, irrespective of the microsatellite status. *Onc Immunology*. 2019;8:e1562834.
- Wischhusen J, Friese MA, Mittelbronn M, et al. HLA-E protects glioma cells from NKG2D-mediated immune responses *in vitro*: implications for immune escape *in vivo*. *J Neuropathol Exp Neurol*. 2005;64:523–8.
- Derré L, Corvaisier M, Charreau B, et al. Expression and release of HLA-E by melanoma cells and melanocytes: potential impact on the response of cytotoxic effector cells. *J Immunol*. 2006;177:3100–7.
- Levy EM, Bianchini M, Von Euw EM, et al. Human leukocyte antigen-E protein is overexpressed in primary human colorectal cancer. *Int J Oncol*. 2008;32:633–41.

14. Braud VM, Allan DSJ, O'Callaghan CA, et al. HLA-E binds to natural killer cell receptors CD94/NKG2A, B and C. *Nature*. 1998;391:795–9.
15. Borrego F, Masilamani M, Marusina AI, et al. The CD94/NKG2 family of receptors: from molecules and cells to clinical relevance. *Immunol Res*. 2006;35:263–78.
16. Bossard C, Bézieau S, Matysiak-Budnik T, et al. HLA-E/β2 microglobulin overexpression in colorectal cancer is associated with recruitment of inhibitory immune cells and tumor progression. *Int J Cancer*. 2012;131:855–63.
17. Wang R, Wang M-J, Ping J. Clinicopathological features and survival outcomes of colorectal cancer in young versus elderly: a population-based cohort study of SEER 9 registries data (1988–2011). *Medicine*. 2015;94:e1402.
18. Suraweera N, Duval A, Reperant M, et al. Evaluation of tumor microsatellite instability using five quasimonomorphic mononucleotide repeats and pentaplex PCR. *Gastroenterol*. 2002;123:1804–11.
19. Umar A, Boland CR, Terdiman JP, et al. Revised Bethesda Guidelines for hereditary nonpolyposis colorectal cancer (Lynch syndrome) and microsatellite instability. *J Natl Cancer Inst*. 2004;96:261–8.
20. Gervois N, Labarriere N, Le Guiner S, et al. High avidity melanoma-reactive cytotoxic T lymphocytes are efficiently induced from peripheral blood lymphocytes on stimulation by peptide-pulsed melanoma cells. *Clin Cancer Res*. 2000;6:1459–67.
21. Lee MS, Menter DG, Kopetz S. Right versus left colon cancer biology: integrating the consensus molecular subtypes. *J Natl Compr Canc Netw*. 2017;15:411–9.
22. Mandrekar JN, Mandrekar SJ, Cha SS. Cutpoint determination methods in survival analysis using SAS®. In: *Proceedings of the 28th SAS Users Group International Conference (SUGI) 2003*, Paper 261–28.
23. André P, Denis C, Soulas C, et al. Anti-NKG2A mAb is a checkpoint inhibitor that promotes anti-tumor immunity by unleashing both T and NK cells. *Cell* 2018;175:1731–1743.e13.
24. Zeestraten ECM, Reimers MS, Saadatmand S, et al. Combined analysis of HLA class I, HLA-E and HLA-G predicts prognosis in colon cancer patients. *Br J Cancer*. 2014;110:459–68.
25. Gooden M, Lampen M, Jordanova ES, et al. HLA-E expression by gynecological cancers restrains tumor-infiltrating CD8+ T lymphocytes. *Proc Natl Acad Sci USA*. 2011;108:10656–61.
26. Gooden MJM, van Hall T. Infiltrating CTLs are bothered by HLA-E on tumors. *Oncoimmunol*. 2012;1:92–3.
27. van Montfoort N, Borst L, Korner MJ, et al. NKG2A blockade potentiates CD8 T cell immunity induced by cancer vaccines. *Cell*. 2018;175:1744–1755.e15.
28. Halama N, Braun M, Kahlert C, et al. Natural killer cells are scarce in colorectal carcinoma tissue despite high levels of chemokines and cytokines. *Clin Cancer Res*. 2011;17:678–89.
29. Sheu B-C, Chiou S-H, Lin H-H, et al. Up-regulation of inhibitory natural killer receptors CD94/NKG2A with suppressed intracellular perforin expression of tumor-infiltrating CD8+ T lymphocytes in human cervical carcinoma. *Cancer Res*. 2005;65:2921–9.
30. Chang W-C, Huang S-C, Tomg P-L, et al. Expression of inhibitory natural killer receptors on tumor-infiltrating CD8+ T lymphocyte lineage in human endometrial carcinoma. *Int J Gynecol Cancer*. 2005;15:1073–80.
31. Zhang L, Zhao Y, Dai Y, et al. Immune landscape of colorectal cancer tumor microenvironment from different primary tumor location. *Front Immunol*. 2018;9:1578.
32. Malmberg K-J, Levitsky V, Norell H, et al. IFN-gamma protects short-term ovarian carcinoma cell lines from CTL lysis via a CD94/NKG2A-dependent mechanism. *J Clin Invest*. 2002;110:1515–23.
33. Chen D, Li L, Zhang X, et al. FOLFOX plus anti-epidermal growth factor receptor (EGFR) monoclonal antibody (mAb) is an effective first-line treatment for patients with RAS-wild left-sided metastatic colorectal cancer: a meta-analysis. *Medicine*. 2018;97:e0097.

## Affiliations

Juliette Eugène<sup>1</sup> · Nicolas Jouand<sup>2,3</sup> · Kathleen Ducoin<sup>2,3</sup> · Delphine Dansette<sup>1</sup> · Romain Oger<sup>2,3</sup> · Cécile Deleine<sup>2,3</sup> · Edouard Leveque<sup>2,3</sup> · Guillaume Meurette<sup>4,5</sup> · Juliette Podevin<sup>4</sup> · Tamara Matysiak<sup>4,5</sup> · Jaafar Bennouna<sup>4,5</sup> · Stéphane Bezieau<sup>5,6</sup> · Christelle Volteau<sup>7</sup> · Wassila El Alami Thomas<sup>8</sup> · Jérôme Chetritt<sup>8</sup> · Olivier Kerdraon<sup>9</sup> · Pierre Fourquier<sup>10</sup> · Emilie Thibaudeau<sup>11</sup> · Frédéric Dumont<sup>11</sup> · Jean-François Mosnier<sup>1,5</sup> · Claire Toquet<sup>1,5</sup> · Anne Jarry<sup>2,3</sup> · Nadine Gervois<sup>2,3</sup> · Céline Bossard<sup>1,2,3,5</sup>

<sup>1</sup> Service d'Anatomie et Cytologie Pathologiques, Centre Hospitalier Universitaire Hôtel Dieu, Nantes, France

<sup>2</sup> CRCINA, INSERM, Université d'Angers, Université de Nantes, Nantes, France

<sup>3</sup> LabEx IGO “Immunotherapy, Graft, Oncology”, Nantes, France

<sup>4</sup> Institut des Maladies de l'Appareil Digestif, Oncologie Digestive, Centre Hospitalier Universitaire Hôtel Dieu, Nantes, France

<sup>5</sup> Université de Nantes, Faculté de Médecine, Nantes, France

<sup>6</sup> Service de Génétique Médicale, Centre Hospitalier Universitaire Hôtel Dieu, Nantes, France

<sup>7</sup> Plateforme de Biométrie, CHU de Nantes, France

<sup>8</sup> Institut d'Histopathologie, Nantes, France

<sup>9</sup> Département de Biologie des Cancers, Institut de Cancérologie de l'Ouest, Nantes, France

<sup>10</sup> Service de Chirurgie Viscérale et Digestive, Hôpital privé du Confluent, Nantes, France

<sup>11</sup> Service d'Oncologie Chirurgicale, Institut de Cancérologie de l'Ouest, Nantes, France